2017 American Control Conference
Sheraton Seattle Hotel
May 24–26, 2017, Seattle, USA

A time-optimal trajectory generation algorithm for quadrotor landing onto a moving platform

Botao Hu[1] and Sandipan Mishra[1]

Abstract— **In this paper, we propose a time-optimal trajectory generation algorithm for landing a 3-DOF (x-z and tilt) quadrotor model onto a moving platform. The algorithm exploits the differential flatness of the quadrotor dynamics model and formulates a nonlinear programming problem, which is then solved to obtain the time-optimal landing trajectory. The advantages of the proposed algorithm over state-of-the-art solution techniques for time-optimal trajectory design include computational efficiency and the ability to incorporate dynamics and state constraints (such as collision avoidance from an obstacle) into the optimization problem. Simulation results and comparisons with a benchmark algorithm show the effectiveness of the proposed method.**

I. INTRODUCTION

Of late, small unmanned aerial vehicles (UAVs) such as quadrotors are being used for many applications such as aerial imaging, package delivery, and surveillance. As such, there is now a growing body of literature on a variety of autonomy problems related to UAVs. [1], [2] present recent surveys on advances in algorithm design for guidance and control of UAVs. Designing time-optimal trajectories for maneuvers are important for several applications, including package delivery, search-and-rescue problems, and perching/landing as presented in [3], [4]. Landing, in particular, poses unique challenges for time-optimal trajectory design because of the stringent safety requirements. Furthermore, landing on to a moving deck or surface further compounds this problem. In this paper, we focus on the design of time-optimal trajectory for landing quadrotors onto moving platforms.

Given a known trajectory or set of fixed way points, the time-optimal maneuver problem may be cast as a *time-optimal trajectory following problem* or *motion planning problem*, which has seen substantial research interest. These problems for different applications, including robotic arms and quadrotors, have been studied in [5]–[8].

However, for most UAV (quadrotor) maneuvers, the trajectory (or waypoints) is not typically given *a priori*. Usually, the initial state of the quadrotor is known and the final state is prescribed but may be time varying as presented in [3], [9]. In this paper, we focus on the problem of time-optimal trajectory generation for a quadrotor landing onto a moving and tilting platform. A key challenge is that the time-optimal trajectory generation algorithm must account for the terminal state being time-varying (and thus dependent on the minimum final time).

[1]Botao Hu and Sandipan Mishra are with the department of Mechanical, Aerospace and Nuclear Engineering of Rensselaer Polytechnic Institute, 110 8th street, Troy, NY, 12180 {hub2,mishs2}@rpi.edu

For this class of problems, a time-optimal trajectory must be generated by solving an optimal control problem. Nonlinear programming algorithms such as Genetic Algorithm [10] and the Switching Time Optimization Algorithm [3] have been proposed.

In addition to directly solving the optimal control problem, an interesting approach that uses differential flatness to address the point-to-point maneuver problem was presented in [4], [11]–[14]. Although this approach does not directly deal with the problem of trajectory generation for landing onto a *moving* (translating and tilting) platform, it presents a mechanism to transform the constraints on the system input onto the constraints on the trajectory by exploiting the differential flatness of the quadrotor dynamics. This approach can significantly improve the computational efficiency of solving the time-optimal point-to-point trajectory generation problem as well as collision avoidance problems as shown in [4].

Inspired by this body of previous work, this paper presents a new trajectory generation algorithm that can generate a time-optimal trajectory to land a quadrotor onto a translating and tilting platform. The general idea is to formulate an optimization problem that exploits the differential flatness property as in [4]. Unlike the algorithm proposed in [4], the formulation of the problem and the selection of the optimization variables presented in this paper expands the scope of problems that may be solved, as explained below.

Specifically, one major advantage of the proposed algorithm is that it allows for the final desired state to be time varying, as long as the final desired state can be expressed as a known explicit function of time (i.e. $\mathbf{x}_d(t) = f(t)$). We demonstrate the applicability of this algorithm for a quadrotor landing/perching onto a translationally moving and tilting platform. Furthermore, this algorithm can also easily incorporate the time-varying obstacle avoidance constraints into the trajectory generation.

This paper is organized as follows. Section II presents the system dynamics and the time-optimal landing problem formulation. Section III develops the differentially flat time-optimal trajectory generation algorithm, while section IV presents the results that illustrate the performance of the algorithm. Section V concludes the paper.

II. 3-DOF Quadrotor Dynamics Model and Problem Formulation

We first present the 3-DOF system dynamics model for a quadrotor and formulate the time-optimal landing trajectory design as a constrained optimization problem.

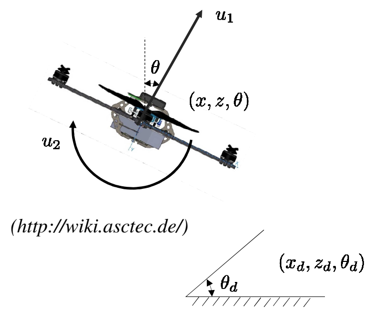

Fig. 1. Schematic of the quadrotor and the landing platform. The quadrotor is modeled with position and pitch angle (x, z, θ) and has two inputs u_1 and u_2. The platform is modeled with $x-z$ position and pitch angle (x_d, z_d, θ_d).

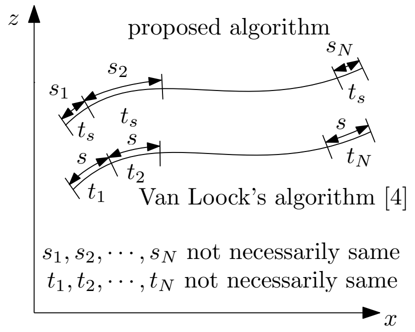

z
proposed algorithm
s_1
s_2
s_N
t_s
t_s
t_s
s
s
s
t_1
t_2
t_N
Van Loock's algorithm [4]
$s_1, s_2, \cdots, s_N$ not necessarily same
$t_1, t_2, \cdots, t_N$ not necessarily same
x

Fig. 2. This is the comparison of trajectory discretization between proposed method and the Van Loock's algorithm proposed in [4]. The duration time for the proposed algorithm is same for each discretized step, while the amount of distance for each step is different. The Van Loock's algorithm adopts an opposite discretize approach.

A. 3-DOF Quadrotor model

The model used in this paper is a two-dimensional three degrees of freedom (3-DOF) quadrotor model, as presented in [3] [4] [1]. The state of the system includes the horizontal position $x(t)$, the vertical height $z(t)$ and the pitch angle $\theta(t)$. $x_d(t), z_d(t), \theta_d(t)$ denote the horizontal position, vertical position and pitch angle of a platform that the quadrotor must land on. Note that the platform state can be *time-varying* but must be explicitly written as a function of time t. Fig. 1 shows the quadrotor and platform models. The state of the quadrotor $\mathbf{x}$ and the state of the platform $\mathbf{x}_d$ can therefore be defined as:

$$\begin{aligned}\mathbf{x} &= \begin{bmatrix} x_1 & x_2 & x_3 & x_4 & x_5 \end{bmatrix} = \begin{bmatrix} x & \dot{x} & z & \dot{z} & \theta \end{bmatrix} \in \mathbb{R}^5 \\ \mathbf{x}_d &= \begin{bmatrix} x_d & \dot{x}_d & z_d & \dot{z}_d & \theta_d \end{bmatrix} \in \mathbb{R}^5. \end{aligned} \quad (1)$$

The thrust is F_t and the mass of the quadrotor is m. The rotation speed is ω. Define the system input $\mathbf{u}$ as:

$$\mathbf{u}(t) = \begin{bmatrix} u_1 \\ u_2 \end{bmatrix} = \begin{bmatrix} \frac{F_T}{m} \\ \omega \end{bmatrix} \in \mathbb{R}^2. \quad (2)$$

The dynamics are thus described by the following:

$$\dot{\mathbf{x}} = \begin{bmatrix} \dot{x}_1 \\ \dot{x}_2 \\ \dot{x}_3 \\ \dot{x}_4 \\ \dot{x}_5 \end{bmatrix} = f(\mathbf{x}, \mathbf{u}) = \begin{bmatrix} x_2 \\ u_1 \sin(x_5) \\ x_4 \\ u_1 \cos(x_5) - g \\ u_2 \end{bmatrix}, \quad (3)$$

where g is the gravitational acceleration. The input u_1 is the nominal thrust, while the input u_2 is the angular rate, both of which are constrained to a feasible set denoted by $\mathbf{U}$. The actuator saturation constraints on u_1 and u_2 can be written as:

$$\begin{aligned}&\mathbf{u}(t) \in \mathbf{U} = \\ &= \left\{ (u_1, u_2) | \begin{array}{c} u_{1\min} \le u_1 \le u_{1\max} \\ u_{2\min} \le u_2 \le u_{2\max} \\ U_{1\min} \le u_{1\min} \le u_{1\max} \le U_{1\max} \\ U_{2\min} \le u_{2\min} \le u_{2\max} \le U_{2\max} \end{array} \right\}. \end{aligned} \quad (4)$$

The actuation range for u_1 is $[U_{1\min}, U_{1\max}]$, while the actuation range for u_2 is $[U_{2\min}, U_{2\max}]$. In order to conservatively design the inputs, we use a smaller range $[u_{i\min}, u_{i\max}]$ for each input. This is in order to account for unknown dynamics and disturbances during operation. Thus, for the trajectory generation, constraints as $u_1 \in [u_{1\min}, u_{1\max}], u_2 \in [u_{2\min}, u_{2\max}]$ are used.

[1]This model is chosen so as to use the results presented in [3] as a benchmark comparison.

B. Problem formulation

Let $\mathbf{g}(\mathbf{x})$ characterize the safety measurables, such as the input or the distance from obstacle, etc. The safety constraints are enforced by staying within a set $\mathbf{G}$, i.e.,:

$$\mathbf{g}(\mathbf{x}) \in \mathbf{G} = \{\mathbf{g} | \mathbf{g}_{\min} \le \mathbf{g}(x) \le \mathbf{g}_{\max}\}. \quad (5)$$

Let t_f be the final (as yet unknown) time, $\mathbf{x}_0$ as the initial state. Denote $\mathbf{x}_d(t_f)$ as the state of the platform at the final time. The time-optimal quadrotor landing problem can be formulated as an optimal control problem. The optimization variables are the system input (over the landing time horizon) and the final landing time. The optimal control problem can be written as (6):

$$\begin{array}{ll} \underset{\mathbf{u}(t), t_f}{\arg\min} & J = t_f \\ s.t & \dot{\mathbf{x}} = f(\mathbf{x}, \mathbf{u}) \\ & \mathbf{x}(t=0) = \mathbf{x}_0 \\ & \mathbf{x}(t=t_f) = \mathbf{x}_d(t_f) \\ & \mathbf{g}(\mathbf{x}(t)) \in \mathbf{G}, \forall t \in [0, t_f] \\ & \mathbf{u}(t) \in \mathbf{U}, \forall t \in [0, t_f]. \end{array} \quad (6)$$

In this paper, we exploit the differentially flat property of the quadrotor system dynamics and reformulate (6) into a nonlinear programming problem. The proposed algorithm discretizes the trajectory into a predetermined number of equal time-segments (N). The distance along the trajectory, s_i, covered in the time-segment $t_i = \Delta t = t_s$ for each step may *vary*. This is the key difference from the Van Loock's algorithm proposed in [4], where for each segment (i) the distance along the trajectory, $s_i = s$, is same, while the length of the time-segment t_i varies. Fig. 2 illustrates this difference in the discretization approaches of these two algorithms.

III. Time-optimal trajectory generation algorithm using differential flatness

In this section, we develop a time-optimal trajectory generation algorithm using differential flatness. The trajectory generation algorithm consists of two key steps: transforming the system dynamics and reformulating the problem into a nonlinear programming problem. The idea behind this is to transform the constraints on the system input into constraints on the system states.

A. System dynamics transformation

In this paper, the system dynamics described by (3) is differentially flat (A formal proof can be found in [4]). The flat output is chosen to be (x,z,θ). The control input u_1 and u_2 at time t can be represented in terms the state from the dynamics equation (3):

$$\begin{bmatrix} 0 \\ u_1(t) \\ u_2(t) \end{bmatrix} = \begin{bmatrix} \cos(\theta) & \sin(\theta) & 0 \\ -\sin(\theta) & \cos(\theta) & 0 \\ 0 & 0 & 1 \end{bmatrix}^{-1} \begin{bmatrix} \ddot{x} \\ \ddot{z}+g \\ \dot{\theta} \end{bmatrix}. \tag{7}$$

Remark: Choosing (x,z,θ) as the flat output simplifies the constraint on u_2 in the optimization problem. The constraint on u_2 can be transformed into a linear constraint of the state $\dot{\theta}$, details of which are presented in the following subsection.

B. Optimization problem formulation

1) Cost function: For the optimization problem, the objective function to be minimized is the total time. The cost function is thus defined same as defined in (6):

$$\min \quad J = t_f. \tag{8}$$

2) Optimization variables: Although the original system dynamics for optimization are continuous, for computational tractability, the system dynamics are discretized into N steps. The number N is a given constant fixed *a priori* . A proper selection of N is a result of trade off between the accuracy and the computational time necessary for the numerical solution of the problem. The sampling time t_s for each step can be calculated from the total time:

$$t_s = \frac{t_f}{N-1}. \tag{9}$$

A discretized state variable $X(k)$ will be used to represent the state variables at k-th sampling time. The elements in $X(k)$ are denoted as $x_k, \dot{x}_k, \cdots, \dot{\theta}_k$:

$$X(k) \; = \; \begin{bmatrix} x_k & \dot{x}_k & z_k & \dot{z}_k & \theta_k & \ddot{x}_k & \ddot{z}_k & \dot{\theta}_k \end{bmatrix}^T \in \mathbb{R}^{8\times 1}. \tag{10}$$

The optimization variables thus include the discretized state variable $X(k)$ for all N steps and the final time t_f. The overall size of the optimization variable is a vector belongs to $\mathbb{R}^{(8N+1)\times 1}$ by summing up all the state variables and final time t_f.

3) Optimization constraints: The optimization constraints may vary for different cases, i.e., collision avoidance, actuator limits, state bounds, etc. Here, we present formulations of some basic classes of constraints.

1) Discretized system kinematics constraints: based on the system discretization, the discretized state variable $X(k)$ must satisfy the following constraints:

$$\begin{bmatrix} x_{k+1} \\ \dot{x}_{k+1} \\ z_{k+1} \\ \dot{z}_{k+1} \\ \theta_{k+1} \end{bmatrix} - \begin{bmatrix} x_k + \dot{x}_k t_s + \frac{\ddot{x}_k t_s^2}{2} \\ \dot{x}_k + \ddot{x}_k t_s \\ z_k + \dot{z}_k t_s + \frac{\ddot{z}_k t_s^2}{2} \\ \dot{z}_k + \ddot{z}_k t_s \\ \theta_k + \dot{\theta}_k t_s \end{bmatrix} = \begin{bmatrix} 0 \\ 0 \\ 0 \\ 0 \\ 0 \end{bmatrix}, \quad \forall k = 1,2,\cdots,N-1, \tag{11}$$

2) System input constraints: based on the differential flatness (7), the constraints on u_1 can be represented as:

$$\begin{aligned} & u_{1\min} \le \ddot{x}_k \sin(\theta_k) + (\ddot{z}_k + g)\cos(\theta_k) \le u_{1\max} \\ & \ddot{x}_k \cos(\theta_k) - (\ddot{z}_k + g)\sin(\theta_k) = 0 \\ & \forall k = 1,2,\cdots,N. \end{aligned} \tag{12}$$

3) Initial and final state constraints: the initial state and the final state of the quadrotor should be same as the given initial state $\mathbf{x}_0$ and the platform final state $\mathbf{x}_d(t_f)$ respectively. The constraints that enforce these are represented as:

$$\begin{aligned} \begin{bmatrix} x_1 & \dot{x}_1 & z_1 & \dot{z}_1 & \theta_1 \end{bmatrix} &= \mathbf{x}_0^T \\ \begin{bmatrix} x_N & \dot{x}_N & z_N & \dot{z}_N & \theta_N \end{bmatrix} &= \mathbf{x}_d(t_f)^T \end{aligned} \tag{13}$$

It should be noted that the platform final state $\mathbf{x}_d(t_f)$ can be time varying if the platform motion can be explicitly expressed as a function of total time t_f.

4) Collision avoidance constraints: it should be noticed that the final state constraint (13) does not avoid collision *during* the landing process. Therefore, a geometric constraint is implemented. Fig. 3 shows the relative position of the quadrotor and the platform. The line CD is the quadrotor and the line AB is the platform. The necessary condition that the quadrotor does not collide with the platform is that the angle θ_1 and θ_2 in Fig. 3 are positive, which can be represented as the cross product of two vectors:

$$\begin{aligned} \vec{CD} \times \vec{CA} &= \begin{bmatrix} 1 \\ \tan(\theta_{dk}) \end{bmatrix} \times \begin{bmatrix} x_k - \frac{L\cos(\theta_k)}{2} - x_{dk} \\ z_k + \frac{L\sin(\theta_k)}{2} - z_{dk} \end{bmatrix} \ge 0 \\ \vec{CD} \times \vec{CB} &= \begin{bmatrix} 1 \\ \tan(\theta_{dk}) \end{bmatrix} \times \begin{bmatrix} x_k + \frac{L\cos(\theta_k)}{2} - x_{dk} \\ z_k - \frac{L\sin(\theta_k)}{2} - z_{dk} \end{bmatrix} \ge 0 \\ & , \forall k = 1,2,\cdots,N. \end{aligned} \tag{14}$$

Given the platform motion can be explicitly defined, the state of the platform $(x_{dk}, z_{dk}, \theta_{dk})$ can be represented as a function of the sampling time t_s.

5) Bounds on the state variables: for the optimization variable $X(k)$, some elements may be bounded (to enforce state bounds or input limits, etc.). These bounds on $X(k)$ are typically linear constraints. Among such bounds: (1) the total time t_f should be positive, (2) the angle of the

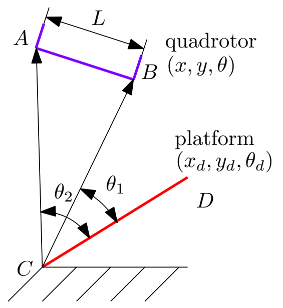

Fig. 3. Plot shows the collision avoidance constraint. L is the length of the quadrotor. By constraining $\theta_1 \geq 0, \theta_2 \geq 0$ will guarentee no collision with the platform.

quadrotor θ_k should be bounded by $[-2\pi, 2\pi]$ and (3) the input $u_2(k) = \dot{\theta}_k$ should be bounded by $[u_{2\min}, u_{2\max}]$ for all $k = 1, 2, \cdots, N$. These constraints are written as

$$\begin{array}{rcl} 0 \leq & t_f & , \\ -2\pi \leq & \theta_k & \leq 2\pi, \\ u_{2\min} \leq & \dot{\theta}_k & \leq u_{2\max}, \\ & \forall k & = 1, 2, \cdots, N. \end{array} \tag{15}$$

4) Formulate the optimization problem: With the definition for the optimization variables, constraints and cost functions, a new formulation of the optimization problem (6) may now be constructed. By stacking the constraints described previously and denote the constraint function as $g(X(k))$, the optimization problem (6) can now be written as

$$\begin{array}{ll} \underset{X(k), t_f}{\arg\min} & J = t_f \\ s.t & g_{\min} \leq g(X(k), t_f) \leq g_{\max} \\ & \forall k = 1, 2, \cdots, N. \end{array} \tag{16}$$

Remark: The optimization problem is modeled using CasADi [15] and solved with Ipopt [16].

C. Trajectory tracking feedback controller design

In the previous subsections, we have designed a time-optimal trajectory. The optimal solution is denoted as $\boldsymbol{X}^*$. Based on the differentially flat property (7), a feedforward control input u_1^*, u_2^* can be obtained. In theory, u_1^* and u_2^* enables trajectory tracking. However, if there is uncertainty in the system dynamics, then directly using the control input from the trajectory will not be effective without a feedback controller. In this subsection, a feedback controller (with the feed-forward control inputs u_1^*, u_2^*) is proposed to track the generated time-optimal reference trajectory.

Define three linearized controls u_x, u_z, u_θ and use u_x, u_z, u_θ as system input to represent u_1 and u_2. The system dynamics can be written as

$$\begin{array}{rcl} \ddot{x} & = & u_1 \sin(\theta) = u_x \\ \ddot{z} & = & u_1 \cos(\theta) - g = u_z \\ \dot{\theta} & = & u_2 = u_\theta \end{array} \tag{17}$$

The system with u_x,u_z,u_θ as input is linear. A state feedback controller is designed for u_x, u_z, u_θ to track the reference trajectory:

$$\begin{array}{rcl} u_x & = & \ddot{x}^* + k_{p1}(x^* - x) + k_{p2}(\dot{x}^* - \dot{x}) \\ u_z & = & \ddot{z}^* + k_{p3}(z^* - z) + k_{p4}(\dot{z}^* - \dot{z}) \\ u_\theta & = & \dot{\theta}^* + k_{p5}(\theta^* - \theta) \end{array} \tag{18}$$

$k_{p1}, k_{p2}, k_{p3}, k_{p4}$ and k_{p4} are positive feedback gains. The system input u_1 can be therefore calculated from u_x, u_z based on (17). Therefore, the controller input can be obtained as:

$$\begin{array}{rcl} u_1 & = & u_x \sin(\theta) + (u_z + g)\cos(\theta) \\ u_2 & = & u_\theta \\ u_1 & \in & [U_{1\min}, U_{1\max}], u_2 \in [U_{2\min}, U_{2\max}] \end{array} \tag{19}$$

By proper selection of the gains, it is possible to achieve relatively good tracking performance.

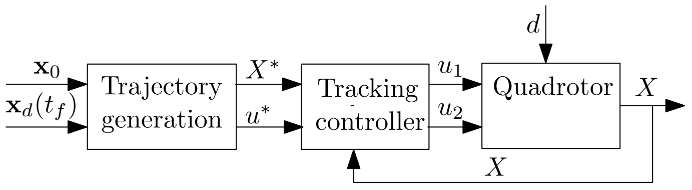

Fig. 4. Block diagram of the overall feedback control structure. In the trajectory generation phase, the initial state and final state is used to generate a reference trajectory $X(k)^*$. In the tracking control phase, a tracking controller is used to generate control input u_1 and u_2 to track the given reference trajectory. d is the disturbance.

IV. Simulation Results

We now present simulation results of trajectory generation for a quadrotor onto a translationally moving and tilting platform. We also present a benchmark comparison with the algorithm described in [3] for several stationary point-to-point maneuvers. For all the simulation results, the input constraints on u_1, u_2 are assumed to be as same as those enforced in the benchmark algorithm [3]:

$$\begin{array}{rcl} \begin{bmatrix} u_{1\min} & u_{1\max} \end{bmatrix} & = & \begin{bmatrix} 1 & 20 \end{bmatrix} m/s^2 \\ \begin{bmatrix} u_{2\min} & u_{2\max} \end{bmatrix} & = & \begin{bmatrix} -10 & 10 \end{bmatrix} rad/s \\ \begin{bmatrix} U_{1\min} & U_{1\max} \end{bmatrix} & = & \begin{bmatrix} 0.5 & 25 \end{bmatrix} m/s^2 \\ \begin{bmatrix} U_{2\min} & U_{2\max} \end{bmatrix} & = & \begin{bmatrix} -15 & 15 \end{bmatrix} rad/s \end{array} \tag{20}$$

All the simulations are performed on an Ubuntu computer with an Intel i7 processor and 16 GB RAM. The algorithm codes are written in Matlab except the simulation of the benchmark comparison which code is written by Python.

A. Benchmark comparison for the trajectory generation algorithm

In this subsection, we compare the time to perform maneuver for the proposed trajectory generation algorithm with benchmark results in [3]. We first perform a series of simulations to pick the best value for the number of trajectory segments to maneuver to $(x_d, z_d, \theta_d) = (15, 0, 0)$. The time to performance maneuver t_f is then compared with the result t_f^* from [3] to obtain the deviation. The deviation is defined as

$$\text{deviation} = \| \frac{t_f - t_f^*}{t_f^*} \| \times 100\% \tag{21}$$

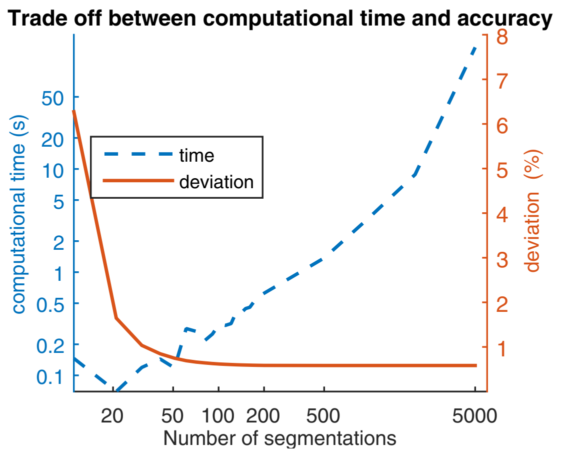

Fig. 5. Plot illustrating the trade off between the accuracy and the computational time. As the number of segments (N) becomes larger, the deviation from the optimal solution obtained in [3] decreases but the computational time increases.

Fig. 5 shows the trade-off between the number of segmentation and the accuracy of the solution obtained. It can be seen that with the increasing resolution of discretization, the computational time increases, while the accuracy of the solution increases. Based on this trade-off, we pick $N = 201$ for all the following simulations.

Next, we compare the time to performance maneuver for 9 cases with the benchmark result in Table. I. The deviations are within $\pm 1\%$ from the benchmark result. The computational time for all cases is less than 1 second. In comparison, the computational time for the benchmark result is on the magnitude of hours [13]. Thus, we claim that this algorithm is computationally efficient and can maintain relatively high accuracy.

B. Landing onto a tilting and moving away platform

This subsection shows the landing of a quadrotor onto a platform that is pitching and moving away. The initial position of the quadrotor is $(x_0, z_0, \theta_0) = (0, 5, 0)$ and the initial horizontal distance is from the quadrotor to the platform is 5 meters. The platform motion is defined as:

$$\begin{bmatrix} x_d(t) & z_d(t) & \theta_d(t) \end{bmatrix} = \begin{bmatrix} 5+t & 0 & -0.3t \end{bmatrix} \tag{22}$$

TABLE I
COST FUNCTION (TIME TO PERFORM MANEUVER, t_f) COMPARISONS WITH THE BENCHMARK ALGORITHM IN [3]

desired terminal position (m, m, rad)	benchmark result (s)	proposed result (s)	deviation (%)	computation time (s)
(0,1,0)	0.650	0.645	-0.78%	0.864
(0,3,0)	1.083	1.084	0.09%	0.722
$(0,5,2\pi)$	1.300	1.298	0.15%	0.903
(3,0,0)	0.890	0.898	0.85%	0.319
(6,0,0)	1.223	1.231	0.65%	0.378
(9,0,0)	1.478	1.488	0.67%	0.342
(12,0,0)	1.694	1.705	0.64%	0.385
(15,0,0)	1.885	1.896	0.58%	0.481
(5,5,0)	1.400	1.4097	0.69%	0.573

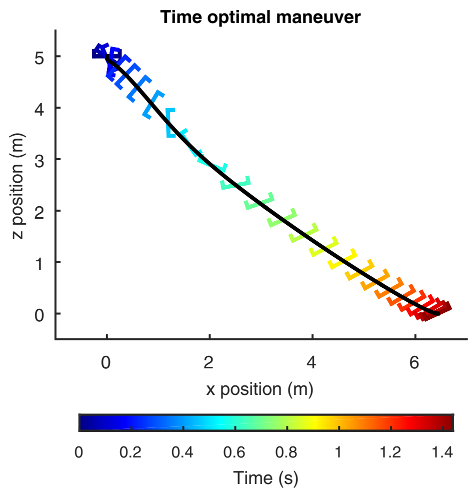

Fig. 6. Trajectory of a quadrotor landing onto a moving platform. The platform is moving away at a constant speed and tilting at a constant speed of 0.3 rad/s. The black line shows the trajectory of the center of the quadrotor and the colored line shows the position and the orientation of the quadrotor every 50 milliseconds.

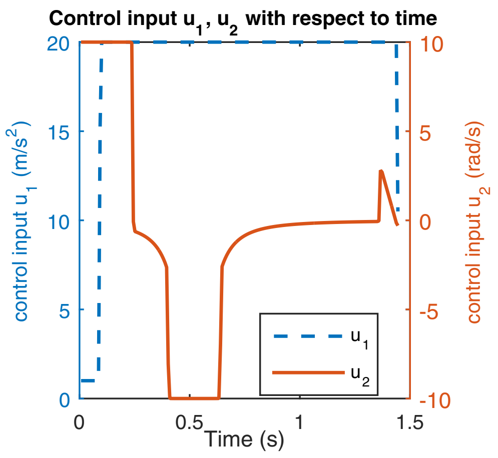

Fig. 7. Plot of the input u_1 and u_2 for the maneuver shown in Fig. 6. It can be seen that u_1 and u_2 switched several times.

Fig. 6 shows the quadrotor maneuver trajectory obtained from the trajectory generation algorithm. The optimal time to land found to be 1.437 seconds. Fig. 7 shows the corresponding input u_1 and u_2 from the optimal solution.

C. Time-optimal maneuver with obstacle avoidance

In this subsection, we demonstrate the performance of the algorithm when the desired terminal position is $(x_d, z_d, \theta_d) = (5, 0, 0)$ while avoiding an obstacle. The obstacle is defined as a circle centered at (2.5,0.75) with a radius of 0.75 meters. Further, we assume that the center of the quadrotor should be at least 1.25 meters away from the center of the obstacle. In this case, additional geometric constraints on the trajectory are added to the trajectory generation problem (16):

$$(x_k - 2.5)^2 + (z_k - .75)^2 - 1.25^2 \geq 0, \forall k = 1, 2, \cdots, N \tag{23}$$

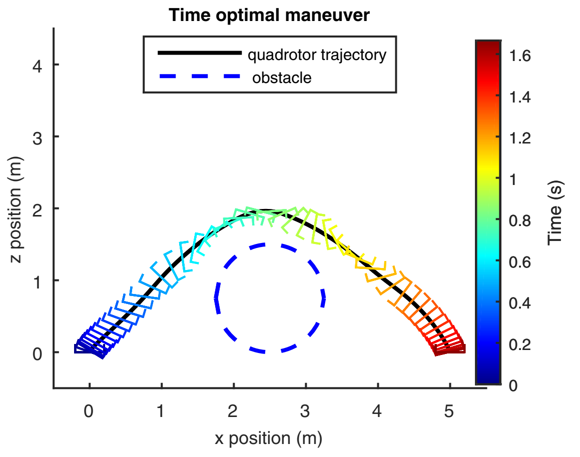

Fig. 8. Plot of quadrotor trajectory for a maneuver that avoids an obstacle, while reaching a fixed position (5,0,0) in a time-optimal manner. The black line is the trajectory of the center of the quadrotor, while the dashed blue line is the obstacle. The colored line shows the quadrotor position and orientation. The quadrotor position is plotted every 70 milliseconds.

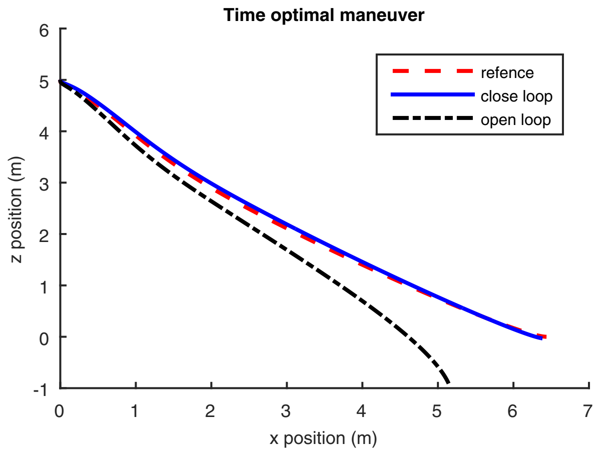

Fig. 9. Plot of the tracking performance for trajectory in Fig. 6 with a feedback controller and an open loop controller. The open loop controller cannot adapt to the difference and it fails to track the reference trajectory . The closed loop controller tracks the reference trajectory well.

Fig. 8 shows the maneuver of the quadrotor. It can be seen that the quadrotor's actual maneuver can avoid collision with the obstacle.

D. Time-optimal maneuver under disturbance

In this subsection, the quadrotor tracks the reference trajectory shown in Fig. 6. We choose the "true" mass of the quadrotor to be 25% larger than the nominal mass, which leads to less acceleration under the same amount of nominal input u_1 according to (2). Fig. 9 shows the trajectories under feedback controller and the open loop controller. From the result, the closed loop controller is able to track the reference trajectory closely while the open loop controller is unable to track the trajectory well.

V. Conclusions and Future Work

In this paper, a time-optimal trajectory generation algorithm for a quadrotor is proposed. By discretizing the system dynamics with a fixed sampling time and applying the differential flatness property of the system dynamics, a standard time-optimal trajectory generation problem is transformed into a nonlinear programming problem. Simulation results and comparison with benchmark algorithm show the effectiveness of the proposed method.

In our future work, we plan to implement the trajectory generation algorithm in a real experimental setup. This method is also promising to be applied for other differentially flat systems, such as car parking problem and the robotic arm motion planning problem.

References

[1] F. Kendoul, "Survey of advances in guidance, navigation, and control of unmanned rotorcraft systems," *Journal of Field Robotics*, vol. 29, no. 2, pp. 315–378, 2012.

[2] J. Sanchez-Lopez, S. Saripalli, P. Campoy, J. Pestana, and C. Fu, "Toward visual autonomous ship board landing of a vtol uav," in *Unmanned Aircraft Systems (ICUAS), 2013 International Conference on*, May 2013, pp. 779–788.

[3] M. Hehn, R. Ritz, and R. DAndrea, "Performance benchmarking of quadrotor systems using time-optimal control," *Autonomous Robots*, vol. 33, no. 1-2, pp. 69–88, 2012.

[4] W. Van Loock, G. Pipeleers, and J. Swevers, "Time-optimal quadrotor flight," in *Proc. of the 2013 European Control Conference (ECC)*, 2013, pp. 1788–1792.

[5] K. Shin and N. McKay, "Minimum-time control of robotic manipulators with geometric path constraints," *IEEE Transactions on Automatic Control*, vol. 30, no. 6, pp. 531–541, 1985.

[6] J. E. Bobrow, S. Dubowsky, and J. Gibson, "Time-optimal control of robotic manipulators along specified paths," *The international journal of robotics research*, vol. 4, no. 3, pp. 3–17, 1985.

[7] R. Verschueren, N. Duijkeren, J. Swevers, and . M. Diehl, "Time-optimal motion planning for n-dof robot manipulators using a path-parametric system reformulation," in *American Control Conference (ACC), 2016*, July 2016, pp. 2092–2097.

[8] D. Verscheure, B. Demeulenaere, J. Swevers, J. De Schutter, and M. Diehl, "Time-optimal path tracking for robots: A convex optimization approach," *IEEE Transactions on Automatic Control*, vol. 54, no. 10, pp. 2318–2327, 2009.

[9] B. Hu, L. Lu, and S. Mishra, "Fast, safe and precise landing of a quadrotor on an oscillating platform," in *American Control Conference, 2015.*, July 2015, pp. 3836–3841.

[10] L.-C. Lai, C.-C. Yang, and C.-J. Wu, "Time-optimal control of a hovering quad-rotor helicopter," *Journal of Intelligent and Robotic Systems*, vol. 45, no. 2, pp. 115–135, 2006.

[11] A. Chamseddine, T. Li, Y. Zhang, C. A. Rabbath, and D. Theilliol, "Flatness-based trajectory planning for a quadrotor unmanned aerial vehicle test-bed considering actuator and system constraints," in *2012 American Control Conference (ACC)*, June 2012, pp. 920–925.

[12] Y. Bouktir, M. Haddad, and T. Chettibi, "Trajectory planning for a quadrotor helicopter," in *Control and Automation, 2008 16th Mediterranean Conference on*, 2008, pp. 1258–1263.

[13] M. Hehn and R. DAndrea, "Real-time trajectory generation for quadrocopters," *IEEE Transactions on Robotics*, vol. 31, no. 4, pp. 877–892, 2015.

[14] W. Van Loock, G. Pipeleers, and J. Swevers, "Optimal motion planning for differentially flat systems with guaranteed constraint satisfaction," in *American Control Conference (ACC), 2015*. IEEE, 2015, pp. 4245–4250.

[15] J. Andersson, "A General-Purpose Software Framework for Dynamic Optimization," PhD thesis, Arenberg Doctoral School, KU Leuven, Department of Electrical Engineering (ESAT/SCD) and Optimization in Engineering Center, Kasteelpark Arenberg 10, 3001-Heverlee, Belgium, October 2013.

[16] A. Wachter and L. Biegler, "On the implementation of a primal-dual interior point filter line search algorithm for large-scale nonlinear programming," *Mathematical Programming*, vol. 106, no. 1, pp. 25–57, 2006.